Fermilab-Conf-03/369

Evaluation of Longitudinal Emittance Growth Caused by Negative Mass Instability in Proton Synchrotrons

J. A. MacLachlan
Fermi National Accelerator Laboratory, * *Box 500, Batavia IL 60510*

Abstract

The theory of negative mass instability (NMI) in proton synchrotrons has been regarded as established for about thirty years, but both accurate calculations and solid beam observations for real cases have been difficult and practically non-existent. The wider availability of so-called computing farms has made credible macroparticle simulations practical for routine use. The comparison of a macroparticle model with the existing theory indicates interesting discrepancies, although the theoretical threshold is confirmed. That comparison and code validation for the model are discussed in the context of useful specific cases. The importance of perturbations other than statistical fluctuation as the seed of instability is considered.

1 INTRODUCTION

Most proton synchrotrons pass through an energy at which the particle circulation frequency is practically independent of momentum differences within beam bunches. At this energy, called the transition energy (E_{T}), $\frac{\partial\omega_{\mathrm{circ}}}{\partial E}$ is zero, changing from positive below E_{T} to negative above. The interparticle repulsion causes charge concentrations within the distribution to disperse below transition but to concentrate above. Just above transition energy, fluctuations in density are practically fixed in the bunch, and the particles in charge surplus regions push one another to higher and lower energy without much change in relative azimuth. If these perturbations of the smooth distribution constitute a sufficient peak current, the resulting field promotes the charge concentration so that the bunch emittance grows significantly within a few beam turns, a disruption called negative mass instability (NMI). There must be a perturbation of ideal smoothness of the charge distribution to start with; the usual assumption is that the statistical fluctuation in the beam current arising from the discreteness of charge carriers is the seed for the instability. However in practice, much stronger perturbations at larger scale are expected. Modeling is an excellent way to explore whether such

*Work supported by the U.S. Department of Energy under contract No. DE-AC02-76CH03000.

microstructure makes an important contribution to instability. A linear perturbation calculation by W. Hardt[1] gives an instability threshold condition and predicts which Fourier components of the beam current will be dominant. Efforts to elucidate the process by macroparticle beam models have been hampered by limits on macroparticle number, effectively limiting the bandwidth to one or two orders of magnitude below the top of the predicted range of unstable Fourier components. The first paper using a macroparticle model to show bunch disruption at about the expected current threshold showed the disrupted distribution to be modulated by the binning frequency.[2] Later attempts with a few hundred to a few thousand times the two thousand macroparticles used in the original effort also evidenced this dubious property. In a recent paper by this author[3], results which did show clustering at less than the binning frequency evidenced some disagreement with the analytic model. However, despite a macroparticle count n_p of $1.2 \cdot 10^7$, the calculation was manifestly statistics limited, and only qualitative conclusions were justified. The ultimate macroparticle model would employ a model particle for each particle in the real bunch. Despite the rapid increase in computing resources available for routine research, this ideal is unlikely to be attained for some years. This paper reports results using at most $n_p = 6.4 \cdot 10^8$ macroparticles to simulate a bunch in the Fermilab Main Injector (FMI) with intensity ranging from $6 \cdot 10^{10}$ to $2 \cdot 10^{11}$ protons in 0.2 eVs. Because these calculations are also statistically marginal, tests have been made to establish the validity of quantitative results.

2 VALIDATION OF MACROPARTICLE MODEL

By increasing the number of macroparticles, the extrapolation between the model and the physical system becomes less extreme. A long-used two dimensional particle tracking code ESME[4] has been converted for parallel processing using MPI (Message Passing Interface). There was little need for global optimization, because for large n_p the computing time is used almost entirely within a single-particle dynamics tracking loop. For $n_p >\sim 10^6$ computing time scaled almost linearly with n_p and was within a few percent of time scaled from single-processor runs of original ESME. A first bench mark was to compare the model to several examples calculated by Ng[5] for the old Fermilab Main Ring. Those instances predicted to be unstable were found to be so in the model. Likewise there was complete agreement on which were stable. Interestingly, marginally stable cases underwent minor high frequency disruption not only above but also below transition. This observation suggests a line of investigation of beam turbulence. Some modification of the code to account for very fast changes in the charge distribution could be needed to follow this lead effectively.

The examples reported hereafter relate to properties of the FMI which is characterized for present purposes by the parameters in Table I. Figure 1 is a plot of emittance growth factor *vs*. initial emittance calculated for FMI bunches of $N = 2 \cdot 10^{11}$ protons using $n_p = 6.4 \cdot 10^8$ macroparticles. The dotted vertical line is the stability threshold according to the perturbation treatment. The results seem almost too consistent with the analytical prediction given the factor of approximately 18 too much discrete charge carrier noise in the model.

There is a heuristic self-bunching model of NMI which gives the same threshold criterion as the perturbation calculation and additionally gives an intuitive idea why the amount of noise in the seed is not a highly critical parameter but the initial bunch emittance is. At wavelengths much shorter

Table 1: Main Injector parameters used in the model

Parameter	Symbol		Units
Circumference	C	3319.42	m
transition energy/$m_\circ c^2$	γ_T	21.84	
rf peak voltage	$V_{\rm rf}$	3.7	MV
rf harmonic	h	588	
beam circulation frequency	$f_\circ$	90.2195	kHz
ramp rate	$\dot{\gamma}$	240.0	s^{-1}
synchronous phase	$\phi_{\rm s}$	42.38	deg
nonadiabatic time	$T_{\rm na}$	1.76	ms
beampipe radius	b	2.5	cm
beam radius	a	0.4	cm
geometric factor	$g_\circ$	4.66	
harmonic of $f_\circ$ for $g = \frac{1}{2}g_\circ$	$n_{1/2}$	2238395	
number of protons per bunch	N	0.6 – $2.0 \cdot 10^{11}$	
average bunch current	$\bar{I}_{\rm bunch}$	0.51 – 1.7	A

than the bunch length, the Fourier spectrum of the beam current is white noise, that is, frequency independent amplitudes independent also of large-scale bunch shape. Calculate the energy extent (bucket height) of the stable oscillation areas separately for each current component and the space charge impedance

$$\frac{Z_\parallel}{n} = -i\frac{Z_\circ g}{2\beta\gamma^2} \quad : \tag{1}$$

$$V_n = Z_\parallel I_n \tag{2}$$

and consequently a microbucket height in eV

$$H_{\mu{\rm B},\,n} = \beta\sqrt{\frac{2eV_nE}{\pi n|\eta|}} \quad , \tag{3}$$

where β and γ are relativistic kinematic parameters, $Z_\circ$ is the free-space impedance of 376.7 Ω, I_n is the $n^{\rm th}$ harmonic peak current, e is the magnitude of the electron charge, E is the total energy of each proton, n is the harmonic number with respect to the beam circulation frequency, and η is the phase slip factor $\gamma_T^{-2} - \gamma^{-2}$. The oscillation in mode n will be unstable if the microbucket height exceeds the bunch height

$$H_{\mu{\rm B},\,n} > H_b \quad . \tag{4}$$

However, because $Z_\parallel$ is proportional to n and $H_{\mu{\rm B},\,n}$ depends on V_n/n, all modes appear to become unstable at the same beam current. The growth rate of the instability is given by the small amplitude oscillation frequency in the microbuckets

$$\lambda_{{\rm rise},\,n} = \sqrt{\frac{n|\eta|eV_n}{2\pi\beta^2E}}f_\circ \quad . \tag{5}$$

Thus, higher frequency modes grow faster and dominate the progress of the disruption. Because the instability appears first at the peak current part of the bunch, the current to be used in calculating

I_n is $\hat{I} = \bar{I}_{\mathrm{bunch}}/B$, where B is the conventional bunching factor. In the high frequency range the current can be thought of as the sum of δ-functions of moving charge so each amplitude has a frequency independent factor of two from the Fourier expansion of the δ-functions. Plausibly, therefore,

$$I_n = 2\bar{I}_{\mathrm{bunch}}/B \ \ , \tag{6}$$

and with this choice the stability threshold criterion of eq. 4 gives the same results as the perturbation calculation. The heuristic model, however, does not include any limit on the action of very high frequency components, although at least one such limiting factor is effective, namely the rolloff of the geometrical factor g. At a harmonic $n_{1/2}$ (see Table I) it is one half of its low frequency value.[1] Nonetheless, one may understand the sharpness of the emittance threshold in terms of whether the microbuckets are higher than the bunch or not and the insensitivity to bandwidth limitation in terms of the simultaneous instability of a wide range of modes. It has been observed in this work that the final bunch disruption is about the same over a wide range of high frequency cutoffs. Even two octaves off the bandwidth indicated in the perturbation calculation gives similar end-state results.

There are some checks which do not rely on matching the stability threshold, mostly of a numerical sort; for example

1. stability with respect to moderate changes in n_p
2. stability with respect to change in seed for random number generator
3. stability with respect to change from time domain to frequency domain calculation
4. bench marking against another code where both are applicable

Not only did these checks provide a measure of reassurance but indicated in addition that results obtained at 4096 bins/rf period were numerically significant even though the macroparticle statistics were marginal at this finest binning employed. The significance of the highest bandwidth results was inferred from a special result concerning $\frac{\mathrm{d}\lambda}{\mathrm{d}t}$ when evaluated by a three-point formula,[6] *viz*., that the numerical noise per bin is the same when the number of bins is doubled if n_p is increased by a factor of 2^3. A sequence of otherwise identical cases was modeled at 512 bins/rf period. In each, n_p was reduced by a factor of eight from the preceding case. From $6.4 \cdot 10^8, n_p$ was reduced in steps to $1.28 \cdot 10^6$, where a difference of a few percent appeared in the strength of the most strongly excited Fourier amplitudes and also in the final emittance. From the fact that the first two reductions in n_p had no significant effect on results, the cubic binning rule implies that 2048 bins are satisfactory with the given n_p, but the step to 4096 bins needed to cover much of the harmonic range of interest according to the perturbation analysis will increase the numerical noise per bin enough to have some effect on results. The differences associated with the final step in the sequence of reductions in n_p are small enough to suggest that results at 4096 bins per rf period are accurate to the few percent level. However, the other checks were made, including runs with different seeds and runs with time domain and frequency domain evaluation of $\frac{\mathrm{d}\lambda}{\mathrm{d}t}$, to confirm this inference. The narrow bandwidth calculation also permitted a direct check on the correctness of the space charge potential calculation. Because the first 256 rf harmonics represent primarily the overall bunch shape but not its finer structure, the voltage calculated by the program for an elliptical distribution was compared to a simple hand calculation. Finally, at n_p accessible to the single processor code ESME, the results were identical with those from the parallel code.

Eq. 5 implies a limitation on macroparticle models which assume that the current distribution remains practically unchanged over a beam turn, a very common ansatz in particle tracking models. The object of study is an instability which causes significant bunch disruption within a small number of beam turns. To extend the calculation to higher frequencies it may become necessary at some point to re-compute the beam current spectrum more than once per turn. However, for the examples used, the rise times are $\mathcal{O}(100)$ beam turns, and the fidelity of the charge distributions should therefore be adequate. However, the adequacy is asserted only, not empirically tested.

There is an *appearance* of disagreement between the linearized perturbation analysis and the model results with respect to the fastest growing mode(s) and with respect to which modes have the greatest integrated power increase. By inspection of plots of mean square amplitudes in bands of 64 harmonics *vs*. time, it appears that in the FMI cases used for Fig. 1, these frequencies both lie lower than predicted.[7] The first should be 117 GHz but is approximately 92 GHz, and the latter should be 67 GHz but is more nearly 49 GHz. The discrepancies could have origin in the high frequency limitation discussed in the preceding paragraph or in the nonlinearity of the equations of motion in the macroparticle model. Extracting a precise comparison from the model is difficult and has not been attempted. However, a time sequence of Fourier spectra given in an earlier paper on this general subject[3] shows the frequencies of dominant amplitudes rapidly shifting downward as the instability develops, thus suggesting the effect of nonlinear equations of motion.

3 FURTHER APPLICATIONS

The results plotted in Fig. 1 have the practical implication that the FMI as currently employed need not be concerned with NMI in establishing a desirable longitudinal emittance regime. On the other hand, the Fermilab Booster injector synchrotron is marginal in this respect at the current performance level, and anticipated improvements need to be developed with NMI limits well understood. Figure 2 shows emittance *vs*. time in the Booster for a realistic charge distribution with some structure which derives from injection conditions. The parameters are those of current best performance. The comparable plot for a distribution smooth but for quasi-random macroparticle distribution is indistinguishable by eye. The only hint of difference between the two distributions is somewhat greater low frequency excitation for the bunch with microstructure early in the development of the instability. An interesting question to be pursued is whether microstructure can seed the instability of a bunch which otherwise would be stable. Although plausible, microstructure driven instability may not be likely because the stability threshold condition is surprisingly strong. NMI is implicated in the emittance growth shown in Fig. 2 by the sudden rise in high frequency beam current components, although it is difficult with only the evidence shown to determine the relative contribution of NMI and single-particle nonlinearity. Figure 3 shows normalized rms Fourier amplitudes for harmonics n= 300 – 319; this plot is chosen as a sample similar to other high frequency bands near 15 GHz. There is an analytic prediction [6] for the emittance growth caused by single-particle nonlinearity which is about 13 % for Booster parameters, appreciably less than seen in this case.

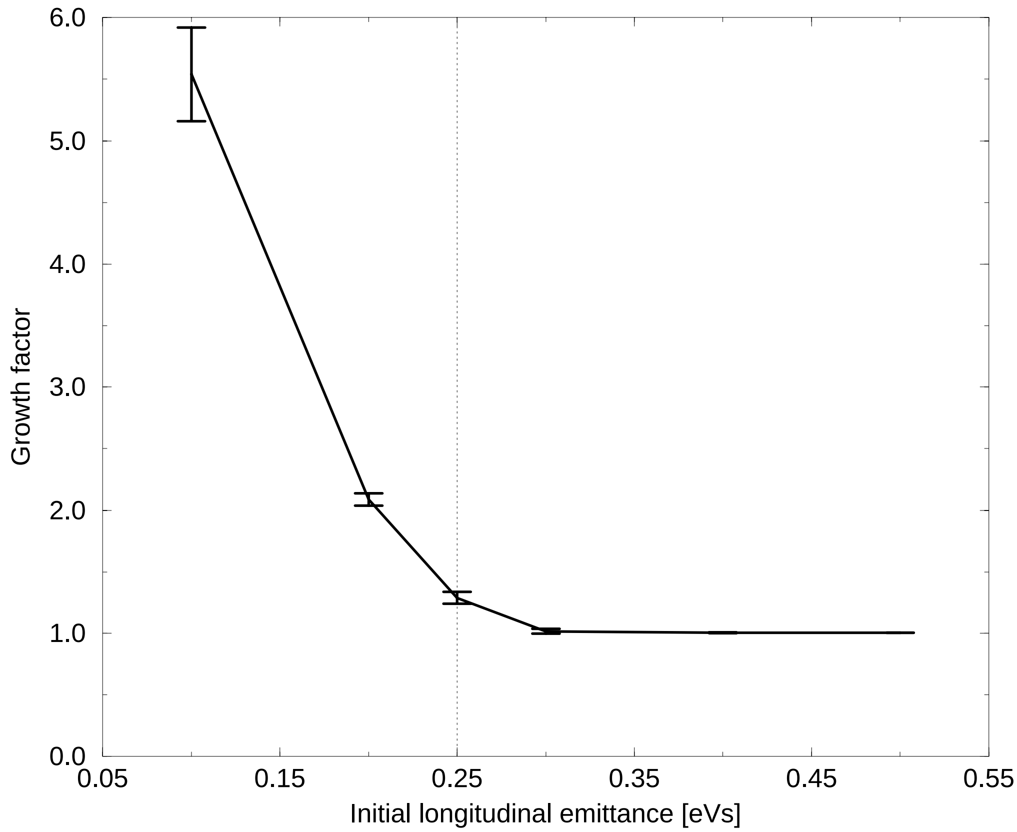

Figure 1: Emittance growth factor *vs*. initial emittance [eVs] for bunches of $2 \cdot 10^{11}$ protons crossing transition in the FMI. Each point is determined by a tracking with $6.4 \cdot 10^8$ macroparticles and a run with 10^8. The statistically weighted mean is the central value with error bars given by the difference between the two runs. The vertical dashed line is the NMI threshold evaluated either from Hardt's[1] formulas or the self-bunching criterion.

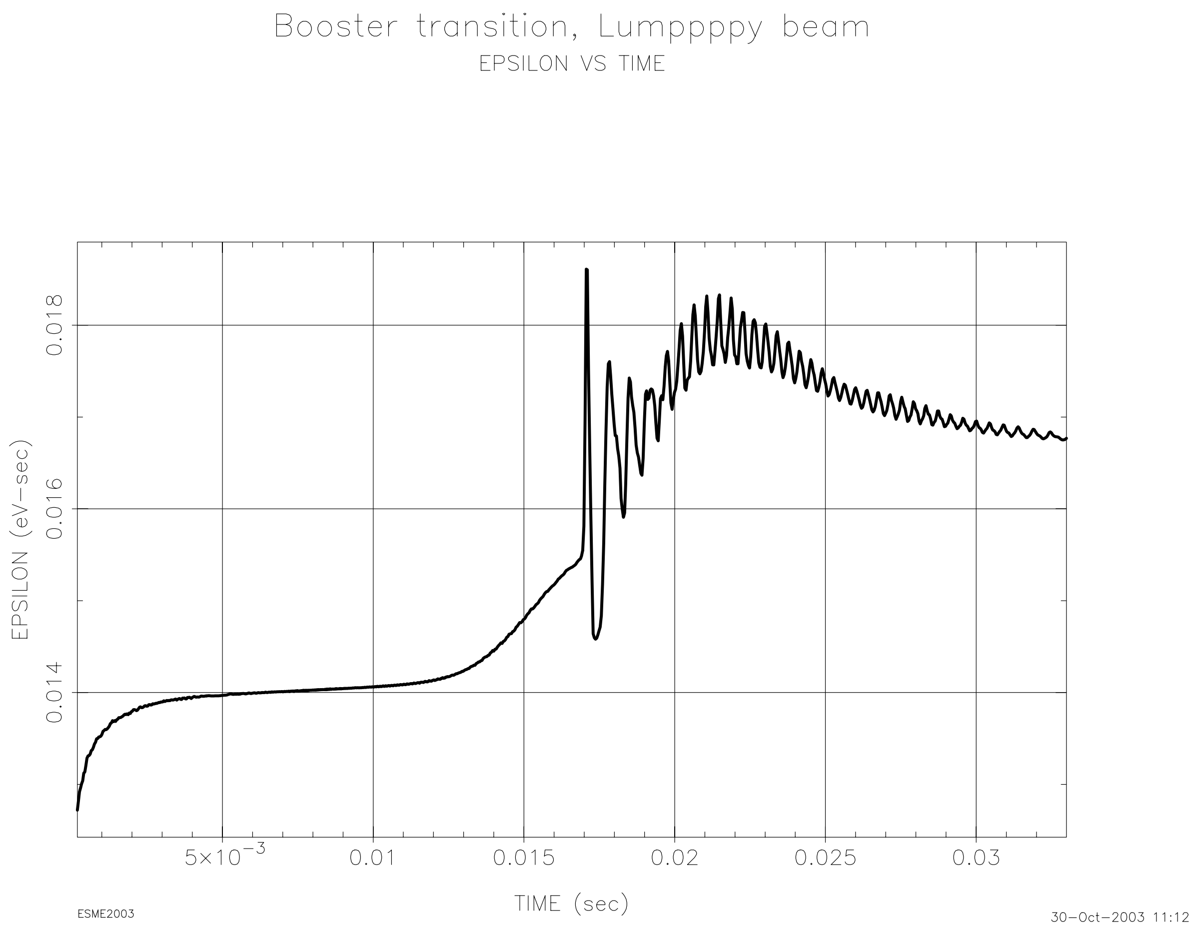

Figure 2: RMS emittance [eVs] *vs*. time [s] for a high intensity ($5 \cdot 10^{12}$ protons total) cycle in the Fermilab Booster injector synchrotron with current typical parameters. The irregularity in the later part of the plot reflects particle loss coming from nonlinear single particle effects in addition to the sudden emittance growth caused by NMI.

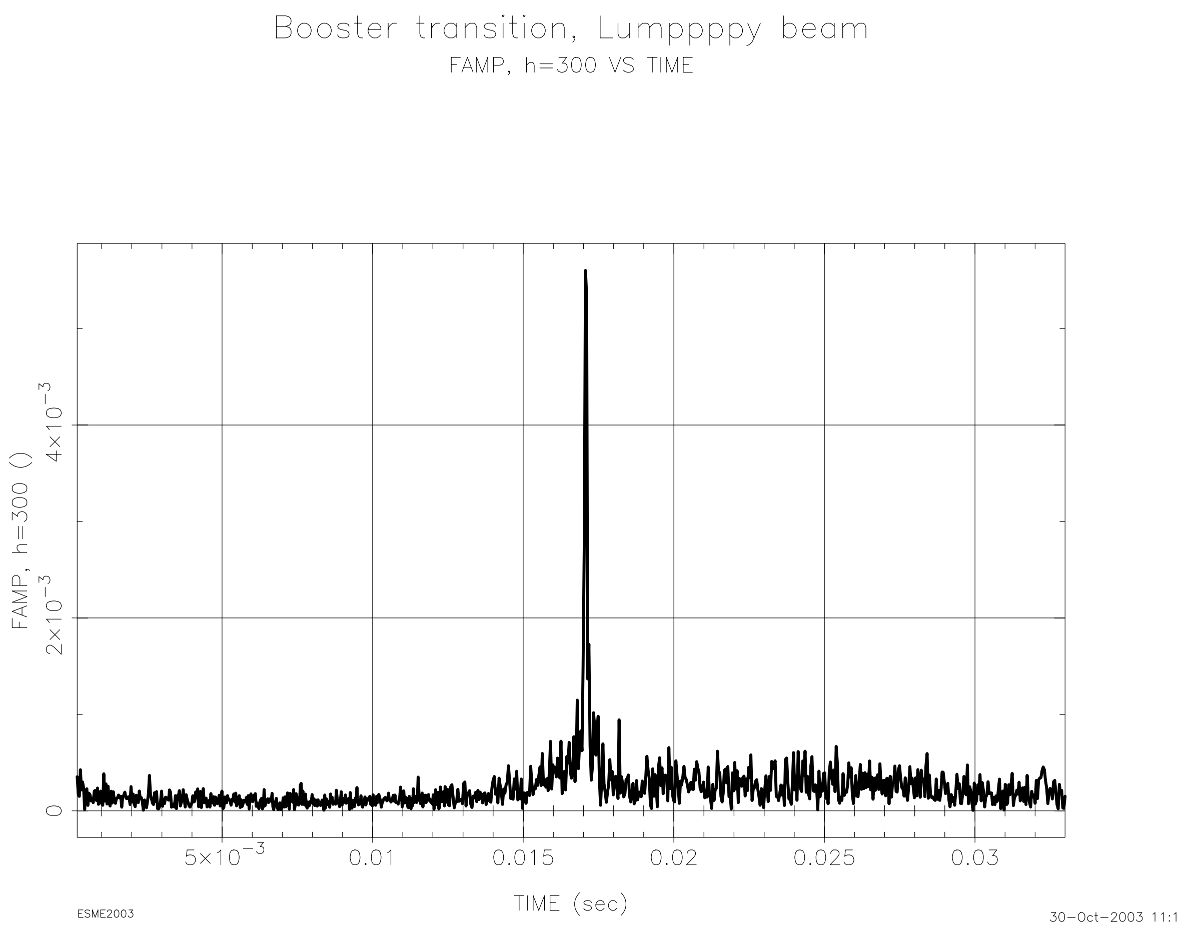

Figure 3: RMS normalized beam charge amplitudes for harmonics n = 300 – 319. The sudden excitation of these amplitudes at transition time 16.8 ms strengthens the argument for NMI as a contributor to the emittance growth seen in Fig. 2, but the relative contributions of NMI and single-particle nonlinearity are difficult to determine.

4 SOFTWARE CONSIDERATIONS

No forefront software technique was required for what is arguably forefront beam physics. Remember, however, that commodity cpu clusters and simple, robust parallel computing software are less than ten years old. In addition, of course, one should credit the open software revolution which has promoted the development of parallel processing software and made commodity clusters economical by eliminating requirements for software licenses for each node. Therefore, it is an important message that yesterday's forefront techniques are already rather widely available, and it has become reasonable for a lone, results-oriented specialist to parallelize a twenty-year-old code in an acceptable time frame. This possibility depends on a conjunction of rather recent trends. Someone with a biggish problem to solve can consider using an MPI framework without serious reservation about additional development time above that required for a purely serial code.

Acknowledgement

My thanks to Jean-François Ostiguy for guidance and encouragement in the parallelization of ESME and general remarks echoed in this talk.

References

[1] Werner Hardt. Gamma-transition-jump scheme of the cps. In $9^{\underline{\mathrm{th}}}$ *Int. Conf. High Energy Accel.*, pages 434–438, Stanford, 1974. SLAC.

[2] W. W. Lee and Lee C. Teng. Beam-bunch length matching at transition crossing. In $8^{\underline{\mathrm{th}}}$ *Int. Conf. High Energy Acc.*, pages 327–330, Geneva, 1971. CERN.

[3] James A. MacLachlan. Multiparticle dynamics in the e-ϕ tracking code esme. In $20^{\underline{\mathrm{th}}}$ *ICFA Adv. Beam Dyn. Workshop*, volume 642 of *AIP Conf. Proc.*, pages 68–70. Fermi National Accelerator Laboratory, American Inst. of Phys., 2002.

[4] James A. MacLachlan. Esme at 18: Realistic numerical modeling of synchrotron motion. In $17^{\underline{\mathrm{th}}}$ *Int. Conf. High Energy Acc.*, Dubna, September 1998. Joint Institute for Nuclear Research.

[5] King-Yuen Ng. Physics of intensity dependent beam instabilities. Physics Note Fermilab-FN-0713, Fermi National Accelerator Laboatory, Batavia IL, 2001.

[6] Jie Wei. *Longitudinal Dynamics of the Non-Adiabatic Regime on Alternatig Gradient Synchrotrons*. PhD thesis, State University of New York (Stony Brook), 1990.

[7] James A. MacLachlan. Macroparticle model for longitudinal emittance growth caused by negative mass instability in a proton synchrotron. Preprint FERMILAB-Pub-03-235 submitted to Phys. Rev. STAB, Sep 2003.